Cite as: Y. Li *et al.*, *Science* 10.1126/science.aaz5425 (2020).

Structural insights into immunoglobulin M

Yaxin Li[1,2]*, Guopeng Wang[3]*, Ningning Li[2,3], Yuxin Wang[1,2], Qinyu Zhu[1,2], Huarui Chu[1,2], Wenjun Wu[4,5], Ying Tan[4,5], Feng Yu[4,5,6], Xiao-Dong Su[1], Ning Gao[2,3], Junyu Xiao[1,2]†

[1]State Key Laboratory of Protein and Plant Gene Research, School of Life Sciences, Peking University, Beijing, China. [2]Peking-Tsinghua Center for Life Sciences, Peking University, Beijing, China. [3]State Key Laboratory of Membrane Biology, School of Life Sciences, Peking University, Beijing, China. [4]Renal Division, Department of Medicine, Peking University First Hospital, Beijing, China. [5]Institute of Nephrology, Peking University, Beijing, China. [6]Department of Nephrology, Peking University International Hospital, Beijing, China.

*These authors contributed equally to this work.

†Corresponding author. Email: junyuxiao@pku.edu.cn

Immunoglobulin M (IgM) plays a pivotal role in both humoral and mucosal immunity. Its assembly and transport depend on the joining chain (J-chain) and the polymeric immunoglobulin receptor (pIgR), but the underlying molecular mechanisms of these processes are unclear. Here we report a cryo-electron microscopy structure of the Fc region of human IgM in complex with the J-chain and pIgR ectodomain. The IgM-Fc pentamer is formed asymmetrically, resembling a hexagon with a missing triangle. The tailpieces of IgM-Fc pack into an amyloid-like structure to stabilize the pentamer. The J-chain caps the tailpiece assembly and bridges the interaction between IgM-Fc and pIgR, which undergoes a large conformational change to engage the IgM–J complex. These results provide a structural basis for the function of IgM.

Immunoglobulin M (IgM) is the first class of antibody produced after B cell activation. Secretory IgM, together with IgA, plays a critical role in the mucosal immune system. IgM forms oligomers, and the presence of multivalent antigen-binding sites in IgM oligomers is a key factor in their ability to agglutinate pathogens. The heavy-chain of IgM contains a C-terminal extension known as the tailpiece that is essential for oligomerization. In the presence of the joining chain (J-chain), a 15-kDa protein that has no homology to other proteins, IgM forms a pentamer, in which five IgM monomers are linked by disulfide bonds between each other and with the J-chain (*1*–*3*). The J-chain also facilitates the dimerization of IgA, which contains a similar tailpiece. The overall structural organization of the IgM pentamer, and the function of J-chain in regulating the assembly processes of these polymeric immunoglobulins, are not completely understood.

Furthermore, to function at the mucosal surface, IgM secreted by the plasma cells has to be transcytosed through the mucosal epithelial cells. This process critically depends on the polymeric immunoglobulin receptor (pIgR) (*4*, *5*). pIgR is a type I transmembrane protein that contains five extracellular immunoglobulin-like domains (D1–D5). It specifically binds to J-chain-containing secretory IgM and IgA at the basolateral surface of epithelial cells and escort them to the apical side. There, the ectodomain is released by proteolysis and secreted together with IgM/IgA. The free ectodomain is often referred to as the secretory component (SC). The molecular mechanism of how pIgR/SC facilitates the secretion of IgM and IgA also remains elusive.

To gain insights into the assembly and secretion of IgM, we reconstituted a tripartite complex containing the Fc region of human IgM (Fcμ), J-chain, and SC (fig. S1), which was then analyzed using cryo-electron microscopy (cryo-EM) (fig. S2). The final constructed model reveals that an IgM Cμ3–Cμ4–tailpiece pentamer and a J-chain molecule form a near-planar structure, and a triangular SC docks perpendicularly to the Fcμ–J plane (Fig. 1). The center region of the structure, including the IgM-Cμ4 domains and tailpieces, the J-chain, and the D1 domain of pIgR/SC, displayed better-than-3-Å resolution, with most of the side chains clearly visualizable (figs. S2 and S3).

Although the structures of individual mouse IgM-Cμ2, IgM-Cμ3, and IgM-Cμ4 domains have been previously characterized (*6*), the structure of an entire Fcμ has yet to be elucidated. In our structure, IgM-Cμ4 forms a dimer within each Fcμ monomer (fig. S4A). The IgM-Cμ4 dimer here highly resembles the dimers formed by IgA-Cα3, IgG-Cγ3, and IgE-Cε4, but is remarkably distinct from the "parallel" dimer observed in the mouse IgM-Cμ4 crystal structure (fig. S4). The IgM-Cμ4 dimer here buries 2,540 Å^2 surface area, larger than the 1,900 Å^2 surface concealed by the mouse IgM-Cμ4 dimer. The physiological significance of these different IgM-Cμ4 dimers remains unclear. The IgM-Cμ3 do-

mains are not involved in direct contacts within each Fcμ monomer (fig. S4A). In some determined structures of IgE, the IgE-Cε2 dimer bends acutely and packs against IgE-Cε3 and IgE-Cε4 (fig. S4E). Based on homology modeling, the IgM-Cμ2 dimer was thought to bend similarly (*7*). However, the densities corresponding to the IgM-Cμ2 dimers, albeit weak, suggest that they do not adopt a stably bent conformation (fig. S4F).

IgM forms a pentamer in the presence of J-chain. Earlier EM studies depicted a stellate appearance of the IgM pentamer with a fivefold symmetry (*8*). Although this model is widely documented in textbooks, a recent negative-stain EM study shows that the IgM pentamer is an asymmetric pentagon with a 50° gap (*9*). A similar gap is present in our structure and is occupied by the J-chain (Fig. 2A). Nevertheless, the gap in our structure has a 61° angle, and the five Fcμ units are arranged in an almost perfect hexagonal symmetry. We speculate that if the J-chain was not present, a sixth Fcμ unit could be readily accommodated to form a hexamer. This is consistent with a recent electron tomography study showing that the IgM pentamer is equivalent to the hexamer except for the J-chain (*10*). IgM-Cμ3 and IgM-Cμ4, as well as the tailpieces all contribute to pentamer formation (Fig. 2A). Cys414 residues from two neighboring IgM-Cμ3 domains are adjacent to one another and likely form interchain disulfide bonds, consistent with earlier analyses (*11*). The FG loops mediate the interaction between two neighboring IgM-Cμ4 domains. Tyr562–Met568 in each tailpiece form a β-strand, and the ten strands are arranged into two five-stranded parallel β-sheets that pack onto one another in an antiparallel fashion. This is reminiscent of the cross-β fibers seen in amyloid proteins and peptides (*12*), and provides the most prominent interactions to stabilize the IgM pentamer. The Tyr562, Val564, Leu566, and Met568 side-chains face inwards and mediate hydrophobic interactions between the two sheets (Fig. 2B and fig. S3A). Mutation of each of these residues either abolished or significantly reduced the oligomerization of mouse IgM (*13*). Val567 residues also stack onto one another to mediate packing interactions between adjacent strands, and mutation of the corresponding Ile567 in mouse IgM disrupted its oligomerization (*13*). Notably, Val567 residues are exposed to the solvent and form extended hydrophobic surface patches (Fig. 2B). The highly conserved Asn563 and Ser565 residues conform to the N-linked glycosylation consensus motif and facilitate the attachment of glycans on Asn563 (Fig. 2B and fig. S3A), which is likely necessary to prevent IgM from forming aggregations. Cys575, the penultimate Cys, mediates the formation of disulfide bonds between adjacent Fcμ monomers, which is a prerequisite for IgM oligomerization (*13*, *14*). Indeed, Cys575^{Fcμ5A} and Cys575^{Fcμ4B} are adjacent to one another, and likely form a disulfide bond (Fig. 3A and fig. S3C). By contrast, Cys575^{Fcμ5B} and Cys575^{Fcμ1A} are linked to the J-chain.

The J-chain was identified almost 50 years ago as an integral subunit of secretory IgA and IgM (*15*, *16*). Guided by the disulfide bond assignments from earlier biochemical studies (*17*), we were able to build an atomic model for the majority of this protein (Fig. 3A and fig. S3B). It interacts with both Fcμ1 and Fcμ5 to seal the Fcμ pentamer. The N-terminal wing comprises four β-strands (β1–β4) and a short helix. The β3 and β4 strands pack on the tailpieces of Fcμ5B and Fcμ1A, respectively, to cap the fiber-like assembly of the IgM tailpieces. Cys14^{J} (superscript J indicates J-chain residues) at the beginning of β2 forms a disulfide bond with Cys575^{Fcμ5B}, and Cys68^{J} in the short helix bonds with Cys575^{Fcμ1A} (Fig. 3A and fig. S3, D and E). The β2–β3 loop also interacts with the base of Fcμ5B. The C-terminal wing contains a long hairpin-like structure, which reaches up to the Cμ3–Cμ4 junction of Fcμ1A and makes extensive hydrophobic contacts (Fig. 3B and fig. S3, F to H). Val113^{J} and P114^{J} interact with Met489^{Fcμ1A}, Pro494^{Fcμ1A}, and Val537^{Fcμ1A}, whereas Leu115^{J}, Val124^{J}, and Thr126^{J} interact with Phe358^{Fcμ1A}, Leu359^{Fcμ1A}, Phe485^{Fcμ1A}, and Val547^{Fcμ1A}. Ala127^{J}, Pro130^{J}, and Tyr134^{J} form a pocket to accommodate Pro544^{Fcμ1A}. Furthermore, this C-terminal hairpin also interacts with pIgR/SC to connect IgM with the receptor.

pIgR/SC binds selectively to IgA or IgM that contains the J-chain (*18*). The D1 domain is the major binding site, and the three loops that are analogous to the complementarity-determining regions (CDRs) of immunoglobulin variable domains are all involved (Fig. 4A) (*19*–*22*). In the ligand-free state of pIgR/SC, D1–D5 are arranged in the form of an isosceles triangle (*22*), with the D2–D3 and D4–D5 sides having similar lengths (Fig. 4B). In the Fcμ–J–SC complex, the D2–D3 side remains unaltered, whereas D1 and D4–D5 undergo drastic conformational changes, leading to the formation of a very different triangular shape (Fig. 4C). D4–D5 rotated 120° en bloc to become co-linear with D2–D3, and the newly formed D3-D4 interface buries a large surface area (1,486 Å^2). D1 rotated 84°, and packs onto D2–D3. This large conformational change is consistent with a previous double electron–electron resonance (DEER) spectroscopy study (*22*). In particular, the distance between the Cα atoms of D1-Thr67 and D5-Gln491 is 78 Å in this new conformation, in good agreement with DEER measurements showing that ligand binding induces a separation of these two residues beyond 70 Å. The three CDRs function as a central hub to mediate a network of interactions with Fcμ1, Fcμ5, and the J-chain (Fig. 4, A, D, and E, and fig. S3, I to N). In CDR1, Val29^{P} (superscript P indicates pIgR/SC residues) interacts with A132^{J} in the J-chain C-terminal hairpin (Fig.

4D). Asn30^{P} forms a hydrogen bond with Arg105^{J}, which in turn packs on Tyr576$^{Fc\mu 5B}$. His32^{P} packs against Tyr134^{J}, which interacts with Pro544$^{Fc\mu 1A}$ as described above. Arg34^{P} forms a salt bridge with Glu468$^{Fc\mu 1B}$. In CDR2 and CDR3, Glu53^{P} interacts with both Arg451$^{Fc\mu 1A}$ and Arg514$^{Fc\mu 1A}$ (Fig. 4E). It has been reported that pIgR from rabbits and rodents transport only IgA, but not IgM (*23*, *24*). Indeed, rabbit pIgR lacks a residue entirely at this position, whereas rodents feature an Asn (*4*, *21*). Arg451 and Arg514 are also not conserved in mouse IgM (fig. S5A). Tyr55^{P} packs against Glu468$^{Fc\mu 1B}$. Asn97^{P} interacts with the main-chain carbonyl group of Leu466$^{Fc\mu 1B}$. Arg99^{P} is sandwiched between Tyr576$^{Fc\mu 5B}$ and Thr574$^{Fc\mu 5A}$. Leu101^{P} interacts with Tyr576$^{Fc\mu 5A}$ and Tyr576$^{Fc\mu 5B}$. Two SC mutants, V29N/R31S and R99N/L101T, which are designed to introduce bulky N-linked glycans in the CDR1 and CDR3 regions, respectively, display greatly reduced interactions with the Fcμ–J complex (Fig. 4F), confirming the functional relevance of the molecular interactions described above.

Two other IgM receptors exist in mammals in addition to pIgR: FcαμR and FcμR/Toso/Faim3 (*25*). They each contains a domain that is homologous to the D1 domain of pIgR. Like pIgR, FcαμR binds both IgA and IgM. Its D1-like domain also shows high sequence similarity to pIgR-D1 (fig. S5B), and residues corresponding to Val29^{P}, Asn30^{P}, His32^{P}, Arg34^{P}, Tyr55^{P}, and Leu101^{P} that are involved in binding to the Fcμ–J complex in pIgR are all present. Thus, FcαμR may interact with IgM in a similar manner as pIgR. FcμR/Toso/Faim3, on the other hand, binds only to IgM. Furthermore, it can interact with both pentameric and hexameric IgM with similar affinities (*26*). This is in contrast to pIgR, which selectively binds to the IgM pentamer that contains the J-chain. Indeed, the D1-like domain of FcμR/Toso/Faim3 is more divergent compared to pIgR-D1 and lacks most of the critical Fcμ–J interacting residues (fig. S5C). Thus, FcμR likely binds IgM in a different fashion.

In summary, we have determined a high-resolution cryo-EM structure of the Fcμ–J–SC complex, which provides a framework for further understanding the functions of IgM, and also sheds light on the interaction between IgM and other receptors. Due to the stronger binding of IgM to its targets, and its more potent activity to induce complement-dependent cytotoxicity, IgM can be potentially exploited for therapeutic applications. Our results pave the way for structure-based engineering of these molecules.

REFERENCES AND NOTES

1. I. N. Norderhaug, F. E. Johansen, H. Schjerven, P. Brandtzaeg, Regulation of the formation and external transport of secretory immunoglobulins. *Crit. Rev. Immunol.* **19**, 481–508 (1999). Medline
2. F. E. Johansen, R. Braathen, P. Brandtzaeg, Role of J chain in secretory immunoglobulin formation. *Scand. J. Immunol.* **52**, 240–248 (2000). doi:10.1046/j.1365-3083.2000.00790.x Medline
3. J. M. Woof, J. Mestecky, Mucosal immunoglobulins. *Immunol. Rev.* **206**, 64–82 (2005). doi:10.1111/j.0105-2896.2005.00290.x Medline
4. C. S. Kaetzel, The polymeric immunoglobulin receptor: Bridging innate and adaptive immune responses at mucosal surfaces. *Immunol. Rev.* **206**, 83–99 (2005). doi:10.1111/j.0105-2896.2005.00278.x Medline
5. H. Turula, C. E. Wobus, The Role of the Polymeric Immunoglobulin Receptor and Secretory Immunoglobulins during Mucosal Infection and Immunity. *Viruses* **10**, 237 (2018). doi:10.3390/v10050237 Medline
6. R. Müller, M. A. Gräwert, T. Kern, T. Madl, J. Peschek, M. Sattler, M. Groll, J. Buchner, High-resolution structures of the IgM Fc domains reveal principles of its hexamer formation. *Proc. Natl. Acad. Sci. U.S.A.* **110**, 10183–10188 (2013). doi:10.1073/pnas.1300547110 Medline
7. D. M. Czajkowsky, Z. Shao, The human IgM pentamer is a mushroom-shaped molecule with a flexural bias. *Proc. Natl. Acad. Sci. U.S.A.* **106**, 14960–14965 (2009). doi:10.1073/pnas.0903805106 Medline
8. A. Feinstein, E. A. Munn, Conformation of the free and antigen-bound IgM antibody molecules. *Nature* **224**, 1307–1309 (1969). doi:10.1038/2241307a0 Medline
9. E. Hiramoto, A. Tsutsumi, R. Suzuki, S. Matsuoka, S. Arai, M. Kikkawa, T. Miyazaki, The IgM pentamer is an asymmetric pentagon with an open groove that binds the AIM protein. *Sci. Adv.* **4**, eaau1199 (2018). doi:10.1126/sciadv.aau1199
10. T. H. Sharp, A. L. Boyle, C. A. Diebolder, A. Kros, A. J. Koster, P. Gros, Insights into IgM-mediated complement activation based on in situ structures of IgM-C1-C4b. *Proc. Natl. Acad. Sci. U.S.A.* **116**, 11900–11905 (2019). Medline
11. F. W. Putnam, G. Florent, C. Paul, T. Shinoda, A. Shimizu, Complete amino acid sequence of the Mu heavy chain of a human IgM immunoglobulin. *Science* **182**, 287–291 (1973). doi:10.1126/science.182.4109.287 Medline
12. D. Eisenberg, M. Jucker, The amyloid state of proteins in human diseases. *Cell* **148**, 1188–1203 (2012). doi:10.1016/j.cell.2012.02.022 Medline
13. D. Pasalic, B. Weber, C. Giannone, T. Anelli, R. Müller, C. Fagioli, M. Felkl, C. John, M. F. Mossuto, C. F. W. Becker, R. Sitia, J. Buchner, A peptide extension dictates IgM assembly. *Proc. Natl. Acad. Sci. U.S.A.* **114**, E8575–E8584 (2017). doi:10.1073/pnas.1701797114 Medline
14. R. Sitia, M. Neuberger, C. Alberini, P. Bet, A. Fra, C. Valetti, G. Williams, C. Milstein, Developmental regulation of IgM secretion: The role of the carboxy-terminal cysteine. *Cell* **60**, 781–790 (1990). doi:10.1016/0092-8674(90)90092-S Medline
15. M. S. Halpern, M. E. Koshland, Noval subunit in secretory IgA. *Nature* **228**, 1276–1278 (1970). doi:10.1038/2281276a0 Medline
16. J. Mestecky, J. Zikan, W. T. Butler, Immunoglobulin M and secretory immunoglobulin A: Presence of a common polypeptide chain different from light chains. *Science* **171**, 1163–1165 (1971). doi:10.1126/science.171.3976.1163 Medline
17. S. Frutiger, G. J. Hughes, N. Paquet, R. Lüthy, J. C. Jaton, Disulfide bond assignment in human J chain and its covalent pairing with immunoglobulin M. *Biochemistry* **31**, 12643–12647 (1992). doi:10.1021/bi00165a014 Medline
18. P. Brandtzaeg, H. Prydz, Direct evidence for an integrated function of J chain and secretory component in epithelial transport of immunoglobulins. *Nature* **311**, 71–73 (1984). doi:10.1038/311071a0 Medline
19. S. Frutiger, G. J. Hughes, W. C. Hanly, M. Kingzette, J. C. Jaton, The amino-terminal domain of rabbit secretory component is responsible for noncovalent binding to immunoglobulin A dimers. *J. Biol. Chem.* **261**, 16673–16681 (1986). Medline
20. R. S. Coyne, M. Siebrecht, M. C. Peitsch, J. E. Casanova, Mutational analysis of polymeric immunoglobulin receptor/ligand interactions. Evidence for the involvement of multiple complementarity determining region (CDR)-like loops in receptor domain I. *J. Biol. Chem.* **269**, 31620–31625 (1994). Medline
21. A. E. Hamburger, A. P. West Jr., P. J. Bjorkman, Crystal structure of a polymeric

immunoglobulin binding fragment of the human polymeric immunoglobulin receptor. *Structure* **12**, 1925–1935 (2004). doi:10.1016/j.str.2004.09.006 Medline

22. B. M. Stadtmueller, K. E. Huey-Tubman, C. J. López, Z. Yang, W. L. Hubbell, P. J. Bjorkman, The structure and dynamics of secretory component and its interactions with polymeric immunoglobulins. *eLife* **5**, e10640 (2016). doi:10.7554/eLife.10640 Medline
23. B. J. Underdown, I. Switzer, G. D. Jackson, Rat secretory component binds poorly to rodent IgM. *J. Immunol.* **149**, 487–491 (1992). Medline
24. M. Røe, I. N. Norderhaug, P. Brandtzaeg, F. E. Johansen, Fine specificity of ligand-binding domain 1 in the polymeric Ig receptor: Importance of the CDR2-containing region for IgM interaction. *J. Immunol.* **162**, 6046–6052 (1999). Medline
25. S. Akula, L. Hellman, The Appearance and Diversification of Receptors for IgM During Vertebrate Evolution. *Curr. Top. Microbiol. Immunol.* **408**, 1–23 (2017). doi:10.1007/82_2017_22 Medline
26. H. Kubagawa, C. M. Skopnik, J. Zimmermann, P. Durek, H.-D. Chang, E. Yoo, L. F. Bertoli, K. Honjo, A. Radbruch, Authentic IgM Fc Receptor (FcμR). *Curr. Top. Microbiol. Immunol.* **408**, 25–45 (2017). doi:10.1007/82_2017_23 Medline
27. D. N. Mastronarde, Automated electron microscope tomography using robust prediction of specimen movements. *J. Struct. Biol.* **152**, 36–51 (2005). doi:10.1016/j.jsb.2005.07.007 Medline
28. S. Q. Zheng, E. Palovcak, J.-P. Armache, K. A. Verba, Y. Cheng, D. A. Agard, MotionCor2: Anisotropic correction of beam-induced motion for improved cryo-electron microscopy. *Nat. Methods* **14**, 331–332 (2017). doi:10.1038/nmeth.4193 Medline
29. K. Zhang, Gctf: Real-time CTF determination and correction. *J. Struct. Biol.* **193**, 1–12 (2016). doi:10.1016/j.jsb.2015.11.003 Medline
30. J. Zivanov, T. Nakane, B. O. Forsberg, D. Kimanius, W. J. Hagen, E. Lindahl, S. H. Scheres, New tools for automated high-resolution cryo-EM structure determination in RELION-3. *eLife* **7**, e42166 (2018). Medline
31. A. Kucukelbir, F. J. Sigworth, H. D. Tagare, Quantifying the local resolution of cryo-EM density maps. *Nat. Methods* **11**, 63–65 (2014). doi:10.1038/nmeth.2727 Medline
32. E. F. Pettersen, T. D. Goddard, C. C. Huang, G. S. Couch, D. M. Greenblatt, E. C. Meng, T. E. Ferrin, UCSF Chimera—A visualization system for exploratory research and analysis. *J. Comput. Chem.* **25**, 1605–1612 (2004). doi:10.1002/jcc.20084 Medline
33. Y. Z. Tan, P. R. Baldwin, J. H. Davis, J. R. Williamson, C. S. Potter, B. Carragher, D. Lyumkis, Addressing preferred specimen orientation in single-particle cryo-EM through tilting. *Nat. Methods* **14**, 793–796 (2017). doi:10.1038/nmeth.4347 Medline
34. M. Biasini, S. Bienert, A. Waterhouse, K. Arnold, G. Studer, T. Schmidt, F. Kiefer, T. Gallo Cassarino, M. Bertoni, L. Bordoli, T. Schwede, SWISS-MODEL: Modelling protein tertiary and quaternary structure using evolutionary information. *Nucleic Acids Res.* **42**, W252–W258 (2014). doi:10.1093/nar/gku340 Medline
35. P. Emsley, B. Lohkamp, W. G. Scott, K. Cowtan, Features and development of Coot. *Acta Crystallogr. D* **66**, 486–501 (2010). doi:10.1107/S0907444910007493 Medline
36. P. D. Adams, P. V. Afonine, G. Bunkóczi, V. B. Chen, I. W. Davis, N. Echols, J. J. Headd, L.-W. Hung, G. J. Kapral, R. W. Grosse-Kunstleve, A. J. McCoy, N. W. Moriarty, R. Oeffner, R. J. Read, D. C. Richardson, J. S. Richardson, T. C. Terwilliger, P. H. Zwart, PHENIX: A comprehensive Python-based system for macromolecular structure solution. *Acta Crystallogr. D* **66**, 213–221 (2010). doi:10.1107/S0907444909052925 Medline

ACKNOWLEDGMENTS

We thank the Core Facilities at the School of Life Sciences, Peking University for help with negative-staining EM; the Cryo-EM Platform of Peking University for help with data collection; the High-performance Computing Platform of Peking University for help with computation; the National Center for Protein Sciences at Peking University for assistance with Amersham Imager; and Guilan Li for help with cDNA library. **Funding:** The work was supported by the National Key Research and Development Program of China (2017YFA0505200, 2016YFC0906000 to J.X.; 2019YFA0508904 to N.G.), the National Science Foundation of China (31570735, 31822014 to J.X.; 31725007, 31630087 to N.G.; 31922036 to N.L.), the Qidong-SLS Innovation Fund to J.X. and N.G.; and the Clinical Medicine Plus X Project of Peking University to J.X. and Y.T. **Author contributions:** Y.L. performed protein purification. Y.L. and G.W. prepared the cryo-EM sample and collected data. G.W. and N.L. processed the cryo-EM data. J.X. and N.G. built the structural model. Y.L. performed the pull-down experiments. J.X. wrote the manuscript, with inputs from all authors. **Competing interests:** The authors declare no competing financial interests. **Data and materials availability:** The cryo-EM map and atomic coordinates of the Fcμ–J–SC complex have been deposited in the EMDB and PDB with accession codes EMD-0782 and 6KXS, respectively. All constructs used for protein expression in this study are available upon request.

SUPPLEMENTARY MATERIALS

science.sciencemag.org/cgi/content/full/science.aaz5425/DC1
Materials and Methods
Figs. S1 to S5
Table S1
References (*27*–*36*)

18 September 2019; accepted 24 January 2020
Published online 6 February 2020
10.1126/science.aaz5425

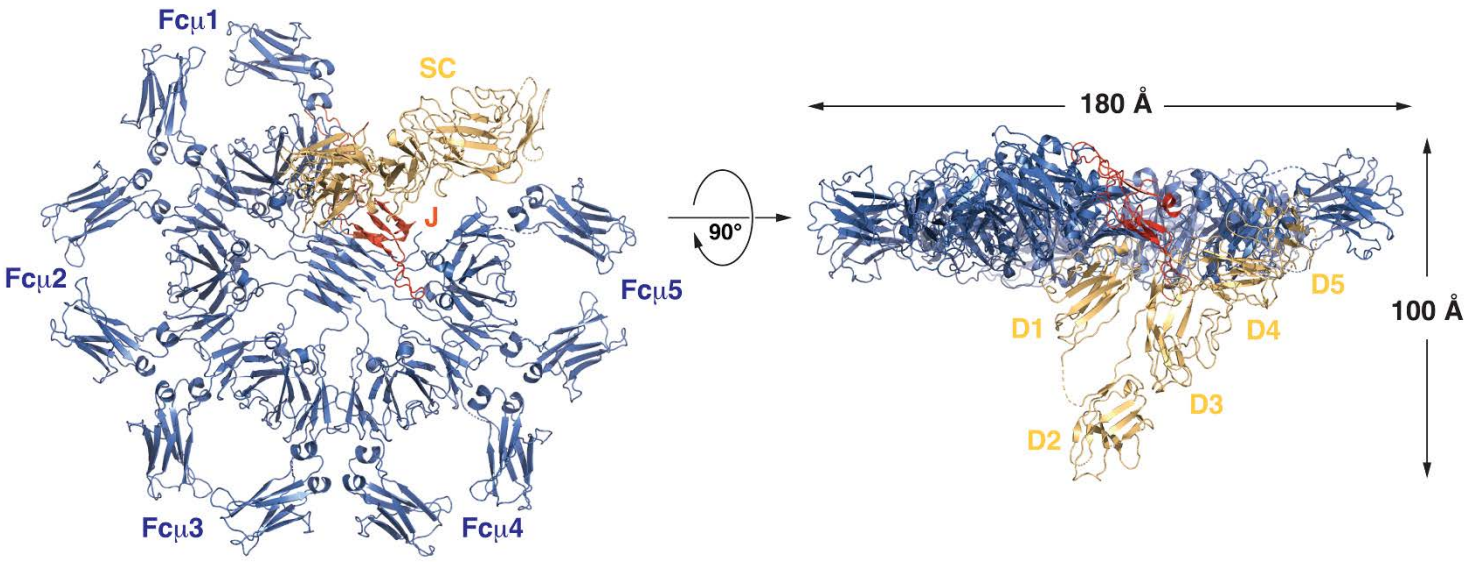

Fig. 1. The cryo-EM structure of the Fcμ pentamer in complex with J-chain and SC. The five Fcμ monomers are shown in blue and labeled Fcμ1–5. The J-chain and SC are shown in red and gold, respectively.

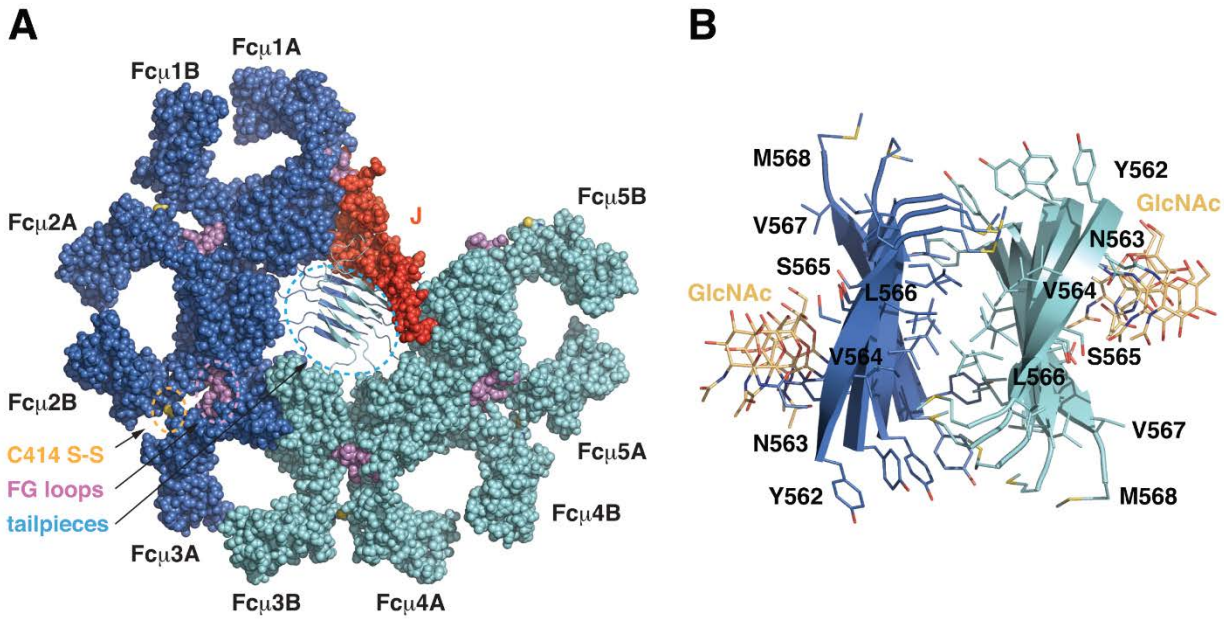

Fig. 2. The Fcμ pentamer. (A) The Fcμ pentamer is shown as a space-filling model except for the tailpieces, which are shown as ribbon diagrams. Five Fcμ chains are shown in blue and five are shown in cyan. The Cys414 disulfide bonds and the FG loops are highlighted. (B) Detailed view of the tailpiece assembly. The N-acetylglucosamine (GlcNAc) molecules attached to Asn563 are shown as orange sticks.

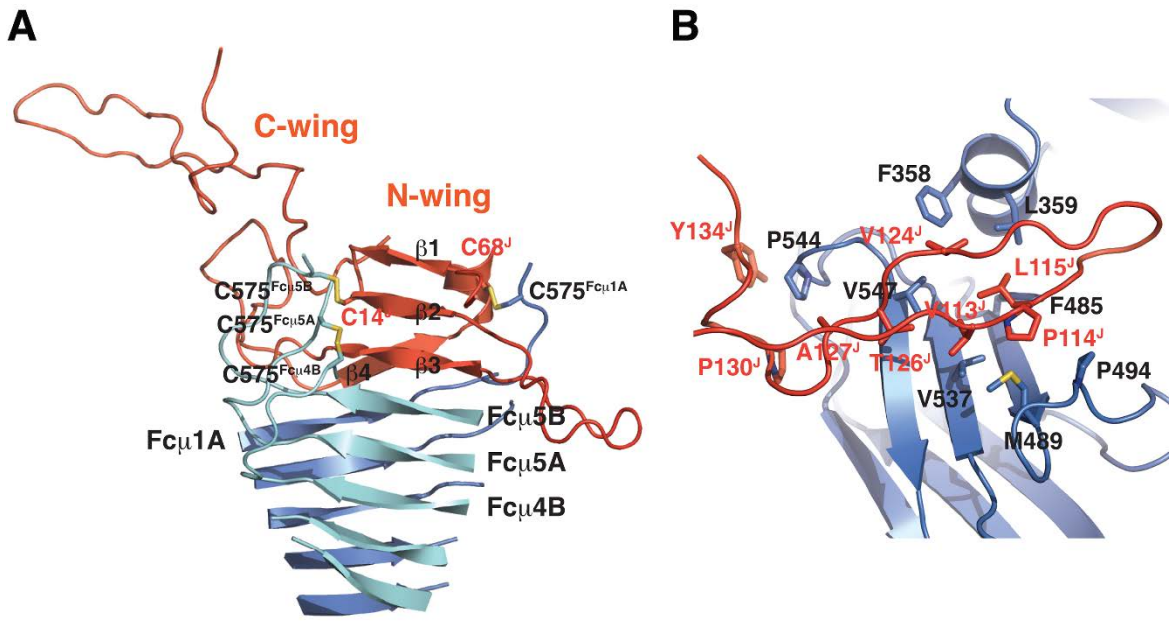

Fig. 3. Structure of the J-chain and its interactions with Fcμ. (**A**) The J-chain has a two-winged structure and interacts with the tailpieces of the Fcμ pentamer. (**B**) The C-terminal hairpin of J-chain interacts with Fcμ1A.

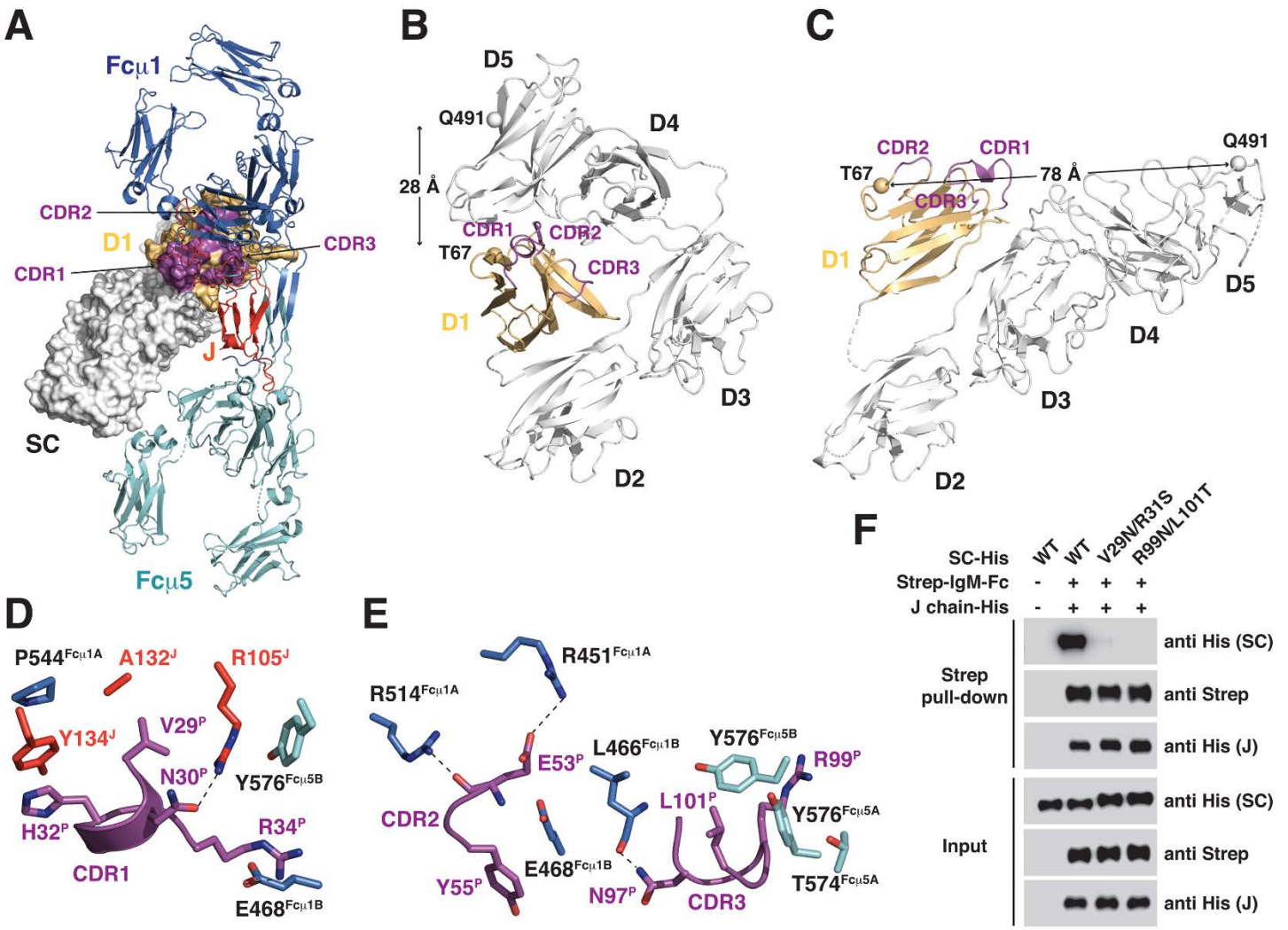

Fig. 4. Conformational change of pIgR/SC and its interaction with the Fcμ–J complex. (**A**) The three CDRs (magenta) in pIgR/SC-D1 (gold) interact with Fcμ1 (blue), Fcμ5 (cyan), and the J-chain (red). pIgR/SC is shown as a surface representation. Its D2–D5 domains are shown in white. (**B**) The structure of apo pIgR/SC (PDB ID: 5D4K). D1 is shown in gold, with the three CDR loops highlighted in magenta. The Cα atoms of D1-T67 and D5-Q491 are shown as spheres, and the distance between them is indicated. (**C**) The structure of pIgR/SC in the Fcμ–J–SC complex. (**D**) Detailed view of the interactions at the D1-CDR1 region. Polar interactions are indicated by dashed lines. (**E**) Detailed view of the interactions at the CDR2 and CDR3 region. (**F**) SC mutants display reduced interactions with Fcμ–J.

Structural insights into immunoglobulin M

Yaxin Li, Guopeng Wang, Ningning Li, Yuxin Wang, Qinyu Zhu, Huarui Chu, Wenjun Wu, Ying Tan, Feng Yu, Xiao-Dong Su, Ning Gao and Junyu Xiao

published online February 6, 2020

Science (print ISSN 0036-8075; online ISSN 1095-9203) is published by the American Association for the Advancement of Science, 1200 New York Avenue NW, Washington, DC 20005. The title *Science* is a registered trademark of AAAS.